Published in final edited form as:
J Neurosurg. 2013 July ; 119(1): 26–36. doi:10.3171/2013.2.JNS12843.

Fast presurgical functional mapping using task-related intracranial high gamma activity:

Laboratory investigation

Tianyi Qian, M.S.[1,2], **Wenjing Zhou, M.D.**[3], **Zhipei Ling, M.D.**[4], **Shangkai Gao, M.S.**[1], **Hesheng Liu, Ph.D.**[2], and **Bo Hong, Ph.D.**[1]

[1]Department of Biomedical Engineering, School of Medicine, Tsinghua University

[2]Athinoula A. Martinos Center for Biomedical Imaging, Department of Radiology, Massachusetts General Hospital, Charlestown, Massachusetts

[3]Department of Neurosurgery and Epilepsy Center, Yuquan Hospital of Tsinghua University

[4]Department of Neurosurgery, Chinese PLA General Hospital, Beijing, China

Abstract

Object—Electrocorticography (ECoG) is a powerful tool for presurgical functional mapping. Power increase in the high gamma band has been observed from ECoG electrodes on the surface of the sensory motor cortex during the execution of body movements. In this study the authors aim to validate the clinical usage of high gamma activity in presurgical mapping by comparing ECoG mapping with traditional direct electrical cortical stimulation (ECS) and functional MRI (fMRI) mapping.

Methods—Seventeen patients with epilepsy participated in an ECoG motor mapping experiment. The patients executed a 5-minute hand/tongue movement task while the ECoG signal was recorded. All 17 patients also underwent extraoperative ECS mapping to localize the motor cortex. Eight patients also participated in a presurgical fMRI study. The high gamma activity on ECoG was modeled using the general linear model (GLM), and the regions showing significant gamma power increase during the task condition compared with the rest condition were localized. The maps derived from GLM-based ECoG mapping, ECS, and fMRI were then compared.

Results—High gamma activity in the motor cortex can be reliably modulated by motor tasks. Localization of the motor regions achieved with GLM-based ECoG mapping was consistent with the localization determined by ECS. The maps also appeared to be highly localized compared with the fMRI activations. Using the ECS findings as the reference, GLM-based ECoG mapping showed a significantly higher sensitivity than fMRI (66.7% for ECoG, 52.6% for fMRI, $p < 0.05$),

Address correspondence to: Bo Hong, Ph.D., Department of Biomedical Engineering, School of Medicine, Tsinghua University, Medical School Building B204, Qinghua Yuan 1, Beijing 100084, China. hongbo@tsinghua.edu.cn.

Disclosure

The work was supported by National Science Foundation of China 61071003 (B. Hong), National Basic Research Program of China 2011CB933204 (B. Hong), and NIH grant K25NS069805 (H. Liu). Tianyi Qian was partly supported by the Postgraduate Study Abroad Program of China Scholarship Council. The authors report no conflict of interest concerning the materials or methods used in this study or the findings specified in this paper.

Author contributions to the study and manuscript preparation include the following. Conception and design: Hong, Gao. Acquisition of data: Qian, Zhou, Ling. Analysis and interpretation of data: Hong, Qian. Drafting the article: Hong, Qian, Liu. Critically revising the article: all authors. Reviewed submitted version of manuscript: all authors. Approved the final version of the manuscript on behalf of all authors: Hong. Statistical analysis: Qian. Administrative/technical/ material support: Hong, Qian, Zhou, Ling. Study supervision: Hong, Gao, Liu.

while the specificity was high for both techniques (> 97%). If the current-spreading effect in ECS is accounted for, ECoG mapping may produce maps almost identical to those produced by ECS mapping (100% sensitivity and 99.5% specificity).

Conclusions—General linear model–based ECoG mapping showed a superior performance compared to traditional ECS and fMRI mapping in terms of efficiency and accuracy. Using this method, motor functions can be reliably mapped in less than 5 minutes.

Keywords

epilepsy surgery; functional mapping; high gamma activity; motor cortex

Information about the anatomical relationship between eloquent cortex and the area to be excised is extremely valuable in neurosurgical treatment. In neurosurgical patients, not only the cortical anatomy but also the locations of functional networks are often distorted due to various pathological changes.[2,20,44,51,55] To map the eloquent cortices, invasive cortical stimulation is often managed perioperatively in the awake patient or in the presurgical patient with subdural grids implanted.[14,23,29,45,60] Presurgical mapping based on ECS is a widely used but time-consuming procedure that often involves an exhaustive search using multiple pairs of electrodes combined with multiple stimulation parameters (for example, current intensity, frequency, pulse width) while patients perform various tasks. According to previous reports,[3,56] 71% of patients receiving ECS may experienced after-discharges and other adverse reactions interfering with accurate mapping.[35]

Functional MRI is another technology commonly used for presurgical functional mapping.[15,25,26,43,50] The basic approach is to conduct an imaging session while a patient performs a task set designed to target a single domain, such as language, memory, or motor function. The obtained images are then analyzed prior to surgery to identify regions of functional activity. Recently the intrinsic fluctuations of the BOLD signal measured by resting-state fMRI have also been suggested as a potential means to localize multiple functional networks simultaneously.[1,8,37] Although the exact relationship between the BOLD signal and electrophysiological activity remains unclear, fMRI is a useful tool, allowing detailed assessment of functional anatomy including the deep brain structures. However, reproducibility of fMRI mapping remains a challenge,[39] and the mapping results are not always consistent with the findings of invasive methods.

While ECS and fMRI both have unique advantages, they also have obvious drawbacks. There is a great clinical need for an optimized presurgical mapping technology that allows fast and precise mapping of the functional networks in individual patients. In epilepsy patients with implanted subdural electrodes, the ECoG signal can provide a direct measure of the neural activity on the brain surface. Various brain functions can modulate the ECoG signal, especially in the high-frequency band. During certain body movement tasks, significant power increase in high gamma oscillations (> 60 Hz)[9,11,30] has been observed. Task-induced or evoked high gamma activity was also reported in the sensory motor cortex,[22,24,28,48] visual cortex,[27,53,57] frontal eye field,[32] and olfactory[42] and speech-related areas.[5,7,10,13,33,38,54,58] The spatial distribution of high gamma activity on ECoG may reveal the functional architecture,[9,11,12] therefore providing an efficient method of presurgical mapping. To map the functional networks using high gamma activity, power spectra density can be calculated and contrasted between the rest and task conditions.[30,36,40,59] However, due to the artifacts from the environment, amplifier, or epileptic discharges, patients often need to execute the task repetitively for a long time in order to attain an adequate signal to noise ratio. Statistical models have been proposed to improve the tolerance to artifacts with various levels of success.[6,49,52]

In this study we attempted to validate the clinical usage of high gamma activity in presurgical mapping by comparing ECoG mapping with traditional direct electrical cortical stimulation (ECS) and fMRI mapping. We developed a novel procedure by modeling the task-related high gamma activity using the general linear model (GLM). As a preliminary exploration, we investigated motor function in 17 surgical candidates. All patients executed a 5-minute task of hand movement and tongue movement while the ECoG signal was recorded. Traditional ECS motor function mapping was also performed in all 17 patients. A task-based fMRI study was performed in 8 of the 17 patients prior to surgery, with the patients performing the same hand and tongue movements as during the ECoG recordings. This multimodal approach allows a direct comparison among these presurgical functional mapping technologies. In terms of both efficiency and accuracy, the performance of the GLM-based ECoG mapping procedure was superior to that of the traditional methods. Using this method, motor functions can be reliably mapped in less than 5 minutes.

Methods

Participants

Seventeen surgical candidates (10 male, 7 female; mean age 18.5 ± 5.2 years) with intractable epilepsy participated in the study. In all cases, temporary placement of subdural electrode arrays (or together with depth electrodes) was scheduled for localization of the epileptic seizure foci. Electrode placement was determined according to the patients' clinical needs. The functional mapping experiments were carried out during stable interictal periods. No seizure had been observed 1 hour before or after the tests in any of the patients. The detailed demographic and clinical information, including the frequency of seizures and placement of the electrodes, is shown in Table 1. Eight patients (those in cases 1–8) participated in the preoperative fMRI test. The study was approved by the ethics committees of the Yuquan Hospital of Tsinghua University and Chinese PLA General Hospital. Written consent was obtained from the patients or their parents in accordance with the guidelines of the hospitals.

Electrical Cortical Stimulation

Direct electrical cortical stimulation was applied to identify motor and somatosensory cortices at the bedside after an adequate number of seizures had been recorded. Using an Ojemann Cortical Stimulator (Integra Life-Sciences), 60-Hz biphasic pulses lasting for 2–5 seconds were delivered to selected pairs of electrodes. The current intensity of the stimulation started at 2 mA and was gradually increased until patients showed or reported symptoms related to the sensory motor cortex or the stimulus strength reached 15 mA.[44]

ECoG Experiment Protocol and Data Analysis

A protocol similar to the conventional fMRI block-design experiment was employed for ECoG functional mapping (Fig. 1 left). Task blocks of 20 seconds' duration were interleaved with 8-second resting blocks. During the task blocks, a picture of a hand or tongue was displayed on the center of the screen for 20 seconds, and the participants were instructed to make a hand or tongue movement as soon as they heard an audio cue (0.2-second duration). Each task block contained only one type of movement. The interval between audio cues was randomized between 3.5 and 4.5 seconds, which resulted in 5 trials of movement for each block. For the hand movement task, the participants were instructed to move only the hand contralateral to the epileptic foci where the electrodes were placed. For the tongue movement task, the participants were instructed to stick out the tongue once. Each task block was repeated 10 times. Therefore the test of a single movement (hand or tongue) took less than 5 minutes.

A long-term video encephalography monitoring system (Bio-logic) was used for the ECoG data recording (1024 Hz/channel, 0.1–134 Hz band-pass filtered). Two electrodes were placed on the scalp as the reference for the ECoG signal. Written instructions were presented on the screen before the experiment started. To synchronize the ECoG recording with the task events, a TTL pulse was delivered to an empty channel of the amplifier through a photocoupler at the beginning of each audio cue.

We modeled the ECoG data using the same approach as is used for modeling of BOLD signal in fMRI studies. [18,19] Equation 1 defines the GLM widely used in fMRI data analysis and was directly adopted for our ECoG modeling.

$$Y=X\beta+\varepsilon \quad \text{Eq. 1}$$

In this model, Y represents the ECoG data band-pass filtered in high gamma band (60–90 Hz, see *Discussion* for details),[46] and X represents the design matrix,[19] which consists of 4 columns corresponding to the hand, tongue, and rest conditions and the constant (Fig. 1 right). Beta (β) represents the model parameter to be estimated using a least square approach, and ε is the estimation error.[19] General linear model fitting provides the t-contrasts for each ECoG electrode, indicating whether it is sensitive to specific movement tasks. The t-contrasts were obtained based on the estimated β and contrast vector c according to Eq. 2, where Std represents standard deviation.

$$t=\frac{c^T\widehat{\beta}}{\mathrm{Std}(c^T\widehat{\beta})} \quad \text{Eq. 2}$$

In fMRI studies, hemodynamic response was modeled by convolving the canonical hemodynamic response function with the events in the experiment. Here we took a similar approach to model the ECoG response. To define an ECoG response function, we fit the high gamma power envelope (0–3 seconds after the task onset) of each patient to a gamma function.[17] The resulting gamma functions were averaged across all 17 cases. The averaged envelope was then taken as the ECoG response function template and convolved with the temporal sequence of the task events (see Fig. 5A for more details). To allow for ease of replication of our study, the software and tools for ECoG data analysis are available upon request.

Functional MRI Experiment Protocol and Data Analysis

The protocol for the fMRI experiment is similar to that of the ECoG experiment described above, except that in the fMRI experiment patients performed self-paced movements without the auditory cue. Patients performed 3 different motor tasks (left hand, right hand, tongue) in 12-second task blocks interleaved with 12-second resting blocks. Each task block contained only one type of movement, and there were 6 blocks for each type of movement in the whole session.

Magnetic resonance images were acquired on the Philips Achieva 3.0-T TX scanner with the 8-channel SENSE head coil. Visual cues were presented during each task block using the Psychophysics Toolbox.[4,31] Structural images were acquired using a sagittal magnetization-prepared rapid gradient echo T1-weighted sequence (TR 2000 msec, TE 2.37 msec, flip angle 90°, slice number 180, 1-mm isotropic voxels). Functional MR images were acquired using echo planar imaging sequences (TR 3000 msec, TE 30 msec, slice number 47, 3-mm isotropic voxels). The fMRI data were processed using SPM8 (Wellcome Trust Centre for Neuroimaging, University College London). The preprocessing included slice timing

correction, rigid body correction for head motion, and normalization for global mean signal intensity across tasks.

Registering ECoG Mapping Results to Presurgical MRI

The ECoG mapping results were registered to the individual's brain structure according to the following steps. 1) Brain surfaces were reconstructed based on the T1-weighted images using the Freesurfer pipeline.[16] 2) Postimplantation CT images were registered to the reconstructed brain surface. We employed a mutual-information–based linear transform to align the MRI and CT in 3D Slicer.[47] Due to brain edema caused by electrode implantation, some electrodes were off the surface when the CT was linearly registered to the preoperative MRI. 3) The 3D pial surface was overlaid with semitransparent CT images using our in-house registration toolbox. This tool allows us to manually adjust the locations of the electrodes according to the grid shape and those electrodes covering the area without edema. As we can visualize the brain structure and electrodes simultaneously, this semiautomatic registration can be finished in approximately 30 minutes for each patient. We compared the electrodes' locations in the intraoperative photos with our registration results according to anatomical landmarks. The registration error of our method was less than 3 mm in all electrodes examined.

For visualization purposes, ECoG electrodes were shown as small spheres (6-mm diameter) on top of the pial surface. The ECoG mapping results were rendered on the cortical surface using the 3D interpolation based on Gaussian smoothing.

Comparing ECoG and fMRI Mapping With ECS Findings

For direct visual comparison among the 3 presurgical mapping modalities, ECS and fMRI results were also plotted on the brain surface. The ECS positive and negative electrodes were marked in yellow and blue, respectively. The fMRI results were mapped on the pial surface using Freesurfer.

Taking the ECS findings as the reference, the sensitivity and specificity of the ECoG mapping and fMRI mapping were quantified. Sensitivity was computed by dividing the number of true positives (ECoG/fMRI positive electrodes that were also positive in ECS) by the true positives plus the number of false negatives (ECoG/ fMRI negative electrodes that were positive in ECS). The specificity was computed by the number of true negatives (ECoG/fMRI negative electrodes that were also negative in ECS) divided by the true negatives plus false positives (ECoG/fMRI positive electrodes that were negative in ECS). In this study, an electrode was defined as positive if the t-contrast was greater than 30 in ECoG mapping or the t-value was greater than 3 in fMRI mapping. The sensitivity and specificity of ECoG mapping were compared with those of fMRI mapping using a paired t-test.

Results

Modulation of High Gamma Activity by Motor Tasks

We first investigated whether high gamma activity could sensitively reflect the brain state changes when patients alternated between the task and rest conditions. Time-frequency analysis was performed to derive the power spectrum of the ECoG signal. The power spectrum during the movement task (from 0.3 to 1.3 seconds after the auditory cue onset) was then contrasted with the power spectrum of the resting period. To illustrate the modulation effect of the task, we selected one representative electrode from each patient based on the ECS findings. The electrode was picked if the patient showed or reported symptoms related to the sensory motor cortex when stimulated with the minimal current

intensity. The power spectra of the representative electrodes were averaged across all 17 patients. We found that the movement tasks induced a significant increase in the high gamma band between 60 and 130 Hz (Fig. 2 left). However, power in the alpha band (8–13 Hz) and beta band (15–30 Hz) demonstrated a decrease during the motor movements. The low gamma band (30–60 Hz) did not show any consistent changes between the task and rest conditions (Fig. 2 left). The observation of these power changes is compatible with previous reports.[6,11,12,36,41]

To determine which frequency band is significantly modulated by the movement task, we performed a statistical test to compare the power spectrum during the movements with the spectrum during the rest. For each frequency bin between 1 Hz and 130 Hz, in increments of 1 Hz, we computed the mean power within the time bins of 15 msec. The power within the bins during the movement tasks and during rest was then analyzed by means of a t-test. Therefore each time-frequency bin during the movement task was assigned a significance level according to its difference from the rest condition. We found that all patients showed significant task/rest difference in the high gamma band and alpha/beta bands. The power spectra in the time-frequency bins showing significant task/rest difference were then averaged across all patients (Fig. 2 right). The modulation effect of the tasks was clearly demonstrated in the high gamma band and some of the low-frequency bands. In addition, we found that the modulation effect in the high gamma band was spatially more localized than the effect in low-frequency bands, consistent with the findings of previous studies.[11,46]

Accurate Mapping of Motor Networks

We tested the accuracy of ECoG mapping by using the ECS findings as the reference. We also compared the results with the noninvasive mapping based on the fMRI activation. The electrodes showing positive findings in the ECS were projected to each individual's brain surface (Fig. 3, left column of each task). The significance values of the ECoG mapping were then rendered on the brain surface for a direct comparison between the 2 modalities (Fig. 3, middle column of each task). The fMRI activation maps were also plotted (Fig. 3, right column of each task). We found that localization of the motor regions by means of GLM-based ECoG mapping was consistent with the regions determined by ECS. The maps also appeared to be highly localized compared with the fMRI activations. Remarkably, ECoG maps were also more localized than ECS findings. One possible cause of this difference is the electrical current spreading effect in cortical stimulation that tends to yield positive findings for electrodes adjacent to the motor area. It may also be related to the difference between the passive movement (stimulation) and the active movement (ECoG). Further investigation is warranted to better understand this difference.

High Sensitivity and Specificity

We then quantified the sensitivity and specificity of the ECoG mapping and fMRI mapping, using the ECS findings as the reference for both (Fig. 4). The sensitivity and specificity of the ECoG and fMRI mapping results are listed in Table 2. We found that both methods showed high specificity (99.6% for ECoG and 97.0% for fMRI). The sensitivity was significantly lower ($p < 0.05$) for fMRI (52.6%) compared with ECoG mapping (66.7%). These results suggest that the performance of ECoG mapping may be superior to that of fMRI mapping. The positive regions in ECoG mapping were highly consistent with the ECS findings. In contrast to ECS, however, ECoG mapping can be accomplished with minimal effort and very rapidly. In our study, motor regions were localized in all patients within 5 minutes.

To simulate the current spreading effect in ECS, we applied a next-neighbor approach to expand the ECoG maps. After this transformation, the sensitivity of ECoG mapping reached

100%, with a specificity of 99.5%, indicating that after smoothing, the GLM-based ECoG mapping was able to generate results almost identical to those obtained with ECS.

Optimization of the Model

In GLM fitting, a critical factor is the selection of the response function template (that is, the hemodynamic response function in fMRI and the ECoG response function in ECoG mapping). In this study, we have employed a template derived from the gamma power envelope of the 17 patients (Fig. 5A). Each trial recorded from the representative electrode (see *Methods*) was fitted to a gamma function (Fig. 5A, blue curves) and the fitted curves were then averaged (Fig. 5A, black curve).

To investigate how the mapping result is affected by the template, we randomly divided the patients into 2 groups and constructed a template based on each group. The motor maps derived from these 2 templates were then compared. We found that the functional maps derived from these 2 templates were nearly identical. The process was repeated 100 times, and we found the mean correlation between the 2 maps derived from the 2 templates was as high as 0.99. Therefore, we concluded that the gamma activity template can be computed from results in a subset of the patient group and applied to other patients. However, we only tested the motor tasks, and it is unclear whether a general response template for higher cognitive functions can be similarly derived from only a few individuals.

The high gamma band covers a broad range of frequencies, and it has been shown that the high gamma power change during tasks is behavior dependent and not uniformly distributed across frequencies.[21] Thus, it is necessary to determine which subband is more sensitive to the motor tasks in the GLM mapping. We divided the high gamma band (60–130 Hz) into subbands with the width of 10 or 30 Hz. The power difference between the task and rest conditions was then calculated for each subband. In addition, the signal-to-noise ratio was estimated for each band. We found that the task/rest power difference was not uniformly distributed in these subbands, and 60–90 Hz appeared to be most sensitive to the task/ rest difference (Fig. 5B). However, the signal-to-noise ratio was at similar levels in all subbands (Fig. 5C).

We then compared the mapping based on our gamma template with results achieved with 2 other templates used in previous explorations.[36,61] The square template is a binary template which sets all time points during the task condition into 1 and the time points in rest condition into 0. This is equal to computing the r square of the power difference between the task and the rest conditions. The peak template keeps the samples between 0.5 and 1.0 seconds (the period with highest gamma activation) and removes all other samples. Comparing the results of representative electrodes derived from these 3 templates, the gamma template yielded greatest significance level (averaged t-value 91), followed by the peak template (averaged t-value 71) and then the square template (averaged t-value 61), when the same number of trials was used. To reach the same t-statistic values by shuffling all trials recorded from the representative electrodes 100 times, on average, 50 trials were needed for the square template, and 29 trials were needed for the peak template, whereas only 20 trials were needed for the gamma template (Fig. 5D). These results indicated that by using the gamma template, we could reduce the testing time by about 60% and 30%, while achieving the same level of sensitivity provided by the square template and the peak template, respectively.

Movement tasks also induce a significant decrease of beta band power.[12] It is therefore interesting to know whether beta band could be used in motor function localization. We found the power change in beta oscillations appeared to be more widespread than in high gamma activation. Using the same GLM approach, we mapped beta band power decreases

in all patients. Compared with the ECS results, mapping using beta power resulted in a sensitivity of 44.2% and a specificity of 92.1%, significantly lower than that of the high gamma mapping and fMRI results.

Discussion

Speed of Mapping in Surgical Planning

The main drawback of ECS is its lengthy procedure. In ECS mapping, testing of at least 10–20 pairs of electrodes is needed, and the current intensity needs to be varied gradually within a certain range (usually 1 mA–15 mA, with increments of 1 mA). It is very common that a single test can take 1–2 hours. The stimulation not only causes fatigue in patients but also entails a risk of after-discharges that occasionally lead to seizures and prevent further mapping of at-risk cortical sites.[3,34] The exhausting nature of ECS makes a retest plan very challenging to both the doctors and the patients involved.

In this study we showed that functional mapping could be accomplished in several minutes with a reasonable accuracy and minimal risk of after-discharge. While ECS mapping must be done with one pair of electrodes at a time, ECoG mapping measures all electrodes at once, significantly reducing the time cost and allowing comprehensive mapping of the covered region. Our results corroborate previous findings that functional mapping can be quickly achieved using ECoG signal.[6,30,36,41]

Compared with other statistical models[52] previously used in ECoG analysis, we found GLM is particularly suitable for modeling the task-related high gamma activity and allows for fast mapping, as demonstrated in our results. The GLM does not require the rejection of a trial if only part of the trial is contaminated by artifacts. The noisy part of the signal can be conveniently excluded while the clean data are kept for the mapping. Therefore reliable maps can be achieved with relatively fewer trials. In our study, we obtained maps with a high significance level even when the ECoG data contained significant amounts of noise caused by head movement or poor contact. With the presence of noise, the maps derived from a 5-minute test were still qualitatively comparable to the ECS results. Another advantage of GLM is that it produces a statistical significance map that differentiates task-related activation from deactivation (for example, the power decrease in alpha and beta band during movement will be reflected by negative t-values in GLM), which is not possible in some models such as SIGFRIED.[52]

High Specificity of Mapping Based on High Gamma Activity

Compared with noninvasive mapping technologies, invasive approaches usually offer a higher spatial resolution. Electrocorticography mapping produces functional maps more similar to ECS results than fMRI mapping. This could be because ECoG and ECS are both based on electrophysiology while fMRI is based on the hemodynamic response. In this study we mapped the function using three modalities in the same individuals; therefore, a direct comparison can be appreciated. A comparison of ECS, ECoG mapping, and fMRI is listed in Table 3.

As the current gold standard, ECS results are usually fairly localized. In our experiment, ECoG electrodes were used to deliver ECS as well and we applied the bipolar cortical stimulation to 2 adjacent ECoG electrodes. The electrical signal creates a circuit between the paired electrodes and the current may spread to neighboring areas. When the current intensity is high, the point spread function of the stimulation may exceed the spatial resolution of ECoG.

Taking the ECS results as the reference, the specificity of the ECoG mapping was 99.5% while the sensitivity was 66.7%. The sensitivity of ECoG mapping was higher than fMRI but still at a low level. However, when we accounted for the current spreading effect in ECS and applied a next-neighbor approach to spatially expand the ECoG maps, the sensitivity of ECoG mapping reached 100%, with a specificity of 99.5%. These results indicated that our fast mapping based on ECoG is qualitatively similar to the ECS mapping, but the maps yielded are potentially more localized.

Caveats

In this study we sought to validate the clinical usage of high gamma activity in presurgical mapping by comparing the ECoG mapping with traditional ECS and fMRI mapping. Our preliminary results implied a great potential for high gamma activity in presurgical mapping. However, several caveats should be emphasized. First, ECoG electrodes only cover part of the brain. It is possible that eloquent cortex is missed by both ECS and ECoG mapping due to insufficient electrode coverage. Thus fMRI mapping has a unique advantage in terms of the completeness of the map (see Case 1 as an example). Using ECS as the gold standard could lead to erroneous conclusions of specificity when the coverage is insufficient. Second, any surgical mapping technology should be subject to final validation with clinical outcomes. In our study, we have only compared our mapping results with ECS in a limited number of patients. The reliability of our approach needs to be further examined with analysis of clinical outcomes in a larger dataset.

Conclusions

High gamma activity in the ECoG signal can be robustly modulated by motor tasks. Electrocorticography mapping based on high gamma activity may provide a very fast approach to mapping out the functional regions in surgical patients. In less than 5 minutes, GLM-based ECoG mapping can yield functional maps comparable to the maps determined by ECS, with higher specificity and sensitivity than fMRI.

Acknowledgments

The authors thank Drs. Yanfang Shi and Dongming Wang at Yuquan Hospital and Dr. Xin Xu at Chinese PLA General Hospital for assistance with cortical stimulation; Drs. Wei Wu and Dan Zhang at Tsinghua University School of Medicine for thoughtful discussion; Drs. Rui Li, Hua Guo, and Xihai Zhao at Tsinghua Biomedical Imaging Center for assistance with MRI.

Abbreviations used in this paper

BOLD	blood oxygen level dependent
ECoG	electrocorticography
ECS	electrical cortical stimulation
fMRI	functional MRI
GLM	general linear model
TTL	transistor-transistor logic

References

1. Biswal B, Yetkin FZ, Haughton VM, Hyde JS. Functional connectivity in the motor cortex of resting human brain using echo-planar MRI. Magn Reson Med. 1995; 34:537–541. [PubMed: 8524021]

2. Bittar RG, Olivier A, Sadikot AF, Andermann F, Pike GB, Reutens DC. Presurgical motor and somatosensory cortex mapping with functional magnetic resonance imaging and positron emission tomography. J Neurosurg. 1999; 91:915–921. [PubMed: 10584835]
3. Blume WT, Jones DC, Pathak P. Properties of after-discharges from cortical electrical stimulation in focal epilepsies. Clin Neurophysiol. 2004; 115:982–989. [PubMed: 15003782]
4. Brainard DH. The psychophysics toolbox. Spat Vis. 1997; 10:433–436. [PubMed: 9176952]
5. Brown EC, Rothermel R, Nishida M, Juhász C, Muzik O, Hoechstetter K, et al. In vivo animation of auditory-language-induced gamma-oscillations in children with intractable focal epilepsy. Neuroimage. 2008; 41:1120–1131. [PubMed: 18455440]
6. Brunner P, Ritaccio AL, Lynch TM, Emrich JF, Wilson JA, Williams JC, et al. A practical procedure for real-time functional mapping of eloquent cortex using electrocorticographic signals in humans. Epilepsy Behav. 2009; 15:278–286. [PubMed: 19366638]
7. Canolty RT, Edwards E, Dalal SS, Soltani M, Nagarajan SS, Kirsch HE, et al. High gamma power is phase-locked to theta oscillations in human neocortex. Science. 2006; 313:1626–1628. [PubMed: 16973878]
8. Cordes D, Haughton VM, Arfanakis K, Wendt GJ, Turski PA, Moritz CH, et al. Mapping functionally related regions of brain with functional connectivity MR imaging. AJNR Am J Neuroradiol. 2000; 21:1636–1644. [PubMed: 11039342]
9. Crone NE, Hao L. The functional significance of event-related spectral changes (ERD/ERS) from the perspective of electrocorticography. Clin Neurophysiol (Suppl). 2002; 54:435–442.
10. Crone NE, Hao L, Hart J Jr, Boatman D, Lesser RP, Irizarry R, et al. Electrocorticographic gamma activity during word production in spoken and sign language. Neurology. 2001; 57:2045–2053. [PubMed: 11739824]
11. Crone NE, Miglioretti DL, Gordon B, Lesser RP. Functional mapping of human sensorimotor cortex with electrocorticographic spectral analysis. II. Event-related synchronization in the gamma band. Brain. 1998; 121:2301–2315. [PubMed: 9874481]
12. Crone NE, Miglioretti DL, Gordon B, Sieracki JM, Wilson MT, Uematsu S, et al. Functional mapping of human sensorimotor cortex with electrocorticographic spectral analysis. I. Alpha and beta event-related desynchronization. Brain. 1998; 121:2271–2299. [PubMed: 9874480]
13. Edwards E, Nagarajan SS, Dalal SS, Canolty RT, Kirsch HE, Barbaro NM, et al. Spatiotemporal imaging of cortical activation during verb generation and picture naming. Neuroimage. 2010; 50:291–301. [PubMed: 20026224]
14. Fandino J, Kollias SS, Wieser HG, Valavanis A, Yonekawa Y. Intraoperative validation of functional magnetic resonance imaging and cortical reorganization patterns in patients with brain tumors involving the primary motor cortex. J Neurosurg. 1999; 91:238–250. [PubMed: 10433312]
15. Fernández G, de Greiff A, von Oertzen J, Reuber M, Lun S, Klaver P, et al. Language mapping in less than 15 minutes: real-time functional MRI during routine clinical investigation. Neuroimage. 2001; 14:585–594. [PubMed: 11506532]
16. Fischl B, Salat DH, Busa E, Albert M, Dieterich M, Haselgrove C, et al. Whole brain segmentation: automated labeling of neuroanatomical structures in the human brain. Neuron. 2002; 33:341–355. [PubMed: 11832223]
17. Friston KJ, Frith CD, Turner R, Frackowiak RS. Characterizing evoked hemodynamics with fMRI. Neuroimage. 1995; 2:157–165. [PubMed: 9343598]
18. Friston KJ, Holmes AP, Poline JB, Grasby PJ, Williams SC, Frackowiak RSJ, et al. Analysis of fMRI time-series revisited. Neuroimage. 1995; 2:45–53. [PubMed: 9343589]
19. Friston KJ, Holmes AP, Worsley KJ, Poline JP, Frith CD, Frackowiak RSJ. Statistical parametric maps in functional imaging: a general linear approach. Hum Brain Mapp. 1995; 2:189–210.
20. Galaburda AM, Rosen GD, Sherman GF. Individual variability in cortical organization: its relationship to brain laterality and implications to function. Neuropsychologia. 1990; 28:529–546. [PubMed: 2203994]
21. Gaona CM, Sharma M, Freudenburg ZV, Breshears JD, Bundy DT, Roland J, et al. Nonuniform high-gamma (60–500 Hz) power changes dissociate cognitive task and anatomy in human cortex. J Neurosci. 2011; 31:2091–2100. [PubMed: 21307246]

22. Gross J, Schnitzler A, Timmermann L, Ploner M. Gamma oscillations in human primary somatosensory cortex reflect pain perception. PLoS Biol. 2007; 5:e133. [PubMed: 17456008]
23. Haglund MM, Berger MS, Shamseldin M, Lettich E, Ojemann GA. Cortical localization of temporal lobe language sites in patients with gliomas. Neurosurgery. 1994; 34:567–576. [PubMed: 7516498]
24. Hauck M, Lorenz J, Engel AK. Attention to painful stimulation enhances gamma-band activity and synchronization in human sensorimotor cortex. J Neurosci. 2007; 27:9270–9277. [PubMed: 17728441]
25. Hirsch J, Ruge MI, Kim KH, Correa DD, Victor JD, Relkin NR, et al. An integrated functional magnetic resonance imaging procedure for preoperative mapping of cortical areas associated with tactile, motor, language, and visual functions. Neurosurgery. 2000; 47:711–722. [PubMed: 10981759]
26. Holodny AI, Schulder M, Liu WC, Wolko J, Maldjian JA, Kalnin AJ. The effect of brain tumors on BOLD functional MR imaging activation in the adjacent motor cortex: implications for image-guided neurosurgery. AJNR Am J Neuroradiol. 2000; 21:1415–1422. [PubMed: 11003273]
27. Hoogenboom N, Schoffelen JM, Oostenveld R, Parkes LM, Fries P. Localizing human visual gamma-band activity in frequency, time and space. Neuroimage. 2006; 29:764–773. [PubMed: 16216533]
28. Ihara A, Hirata M, Yanagihara K, Ninomiya H, Imai K, Ishii R, et al. Neuromagnetic gamma-band activity in the primary and secondary somatosensory areas. Neuroreport. 2003; 14:273–277. [PubMed: 12598745]
29. Jack CR Jr, Thompson RM, Butts RK, Sharbrough FW, Kelly PJ, Hanson DP, et al. Sensory motor cortex: correlation of presurgical mapping with functional MR imaging and invasive cortical mapping. Radiology. 1994; 190:85–92. [PubMed: 8259434]
30. Kirsch HE, Sepkuty JP, Crone NE. Multimodal functional mapping of sensorimotor cortex prior to resection of an epileptogenic perirolandic lesion. Epilepsy Behav. 2004; 5:407–410. [PubMed: 15145312]
31. Kleiner M, Brainard D, Pelli D. What's new in Psychtoolbox-3? Perception. 2007; 36(Suppl):14. (Abstract).
32. Lachaux JP, George N, Tallon-Baudry C, Martinerie J, Hugueville L, Minotti L, et al. The many faces of the gamma band response to complex visual stimuli. Neuroimage. 2005; 25:491–501. [PubMed: 15784428]
33. Lachaux JP, Jerbi K, Bertrand O, Minotti L, Hoffmann D, Schoendorff B, et al. A blueprint for real-time functional mapping via human intracranial recordings. PLoS ONE. 2007; 2:e1094. [PubMed: 17971857]
34. Lesser RP, Lüders H, Klem G, Dinner DS, Morris HH, Hahn J. Cortical afterdischarge and functional response thresholds: results of extraoperative testing. Epilepsia. 1984; 25:615–621. [PubMed: 6479112]
35. Lesser RP, Lüders H, Klem G, Dinner DS, Morris HH III, Hahn J. Ipsilateral trigeminal sensory responses to cortical stimulation by subdural electrodes. Neurology. 1985; 35:1760–1763. [PubMed: 4069367]
36. Leuthardt EC, Miller K, Anderson NR, Schalk G, Dowling J, Miller J, et al. Electrocorticographic frequency alteration mapping: a clinical technique for mapping the motor cortex. Neurosurgery. 2007; 60 (4 Suppl 2):260–271. [PubMed: 17415162]
37. Liu H, Buckner RL, Talukdar T, Tanaka N, Madsen JR, Stufflebeam SM. Task-free presurgical mapping using functional magnetic resonance imaging intrinsic activity. Laboratory investigation. J Neurosurg. 2009; 111:746–754. [PubMed: 19361264]
38. Mainy N, Jung J, Baciu M, Kahane P, Schoendorff B, Minotti L, et al. Cortical dynamics of word recognition. Hum Brain Mapp. 2008; 29:1215–1230. [PubMed: 17712785]
39. McGonigle DJ, Howseman AM, Athwal BS, Friston KJ, Frackowiak RS, Holmes AP. Variability in fMRI: an examination of intersession differences. Neuroimage. 2000; 11:708–734. [PubMed: 10860798]
40. Miller KJ, denNijs M, Shenoy P, Miller JW, Rao RPN, Ojemann JG. Real-time functional brain mapping using electrocorticography. Neuroimage. 2007; 37:504–507. [PubMed: 17604183]

41. Miller KJ, Leuthardt EC, Schalk G, Rao RPN, Anderson NR, Moran DW, et al. Spectral changes in cortical surface potentials during motor movement. J Neurosci. 2007; 27:2424–2432. [PubMed: 17329441]
42. Miyanari A, Kaneoke Y, Ihara A, Watanabe S, Osaki Y, Kubo T, et al. Neuromagnetic changes of brain rhythm evoked by intravenous olfactory stimulation in humans. Brain Topogr. 2006; 18:189–199. [PubMed: 16544208]
43. Mueller WM, Yetkin FZ, Hammeke TA, Morris GL III, Swanson SJ, Reichert K, et al. Functional magnetic resonance imaging mapping of the motor cortex in patients with cerebral tumors. Neurosurgery. 1996; 39:515–521. [PubMed: 8875481]
44. Ojemann G, Ojemann J, Lettich E, Berger M. Cortical language localization in left, dominant hemisphere. An electrical stimulation mapping investigation in 117 patients. J Neurosurg. 1989; 71:316–326. [PubMed: 2769383]
45. Penfield W. The circulation of the epileptic brain. Res Publ Assoc Res Nerv Ment Dis. 1937; 18:605–637.
46. Pfurtscheller G, Graimann B, Huggins JE, Levine SP, Schuh LA. Spatiotemporal patterns of beta desynchronization and gamma synchronization in corticographic data during self-paced movement. Clin Neurophysiol. 2003; 114:1226–1236. [PubMed: 12842719]
47. Pieper S, Halle M, Kikinis R. 3D Slicer. Proc IEEE Int Symp Biomed Imaging. 2004; 1:632–635.
48. Ray S, Niebur E, Hsiao SS, Sinai A, Crone NE. High-frequency gamma activity (80–150Hz) is increased in human cortex during selective attention. Clin Neurophysiol. 2008; 119:116–133. [PubMed: 18037343]
49. Roland J, Brunner P, Johnston J, Schalk G, Leuthardt EC. Passive real-time identification of speech and motor cortex during an awake craniotomy. Epilepsy Behav. 2010; 18:123–128. [PubMed: 20478745]
50. Roux FE, Boulanouar K, Ranjeva JP, Tremoulet M, Henry P, Manelfe C, et al. Usefulness of motor functional MRI correlated to cortical mapping in Rolandic low-grade astrocytomas. Acta Neurochir (Wien). 1999; 141:71–79. [PubMed: 10071689]
51. Sanai N, Mirzadeh Z, Berger MS. Functional outcome after language mapping for glioma resection. N Engl J Med. 2008; 358:18–27. [PubMed: 18172171]
52. Schalk G, Leuthardt EC, Brunner P, Ojemann JG, Gerhardt LA, Wolpaw JR. Real-time detection of event-related brain activity. Neuroimage. 2008; 43:245–249. [PubMed: 18718544]
53. Siegel M, Donner TH, Oostenveld R, Fries P, Engel AK. High-frequency activity in human visual cortex is modulated by visual motion strength. Cereb Cortex. 2007; 17:732–741. [PubMed: 16648451]
54. Sinai A, Bowers CW, Crainiceanu CM, Boatman D, Gordon B, Lesser RP, et al. Electrocorticographic high gamma activity versus electrical cortical stimulation mapping of naming. Brain. 2005; 128:1556–1570. [PubMed: 15817517]
55. Steinmetz H, Fürst G, Freund HJ. Variation of perisylvian and calcarine anatomic landmarks within stereotaxic proportional coordinates. AJNR Am J Neuroradiol. 1990; 11:1123–1130. [PubMed: 2124038]
56. Szelényi A, Joksimovic B, Seifert V. Intraoperative risk of seizures associated with transient direct cortical stimulation in patients with symptomatic epilepsy. J Clin Neurophysiol. 2007; 24:39–43. [PubMed: 17277576]
57. Tallon-Baudry C, Bertrand O, Hénaff MA, Isnard J, Fischer C. Attention modulates gamma-band oscillations differently in the human lateral occipital cortex and fusiform gyrus. Cereb Cortex. 2005; 15:654–662. [PubMed: 15371290]
58. Towle VL, Yoon HA, Castelle M, Edgar JC, Biassou NM, Frim DM, et al. ECoG gamma activity during a language task: differentiating expressive and receptive speech areas. Brain. 2008; 131:2013–2027. [PubMed: 18669510]
59. Wu M, Wisneski K, Schalk G, Sharma M, Roland J, Breshears J, et al. Electrocorticographic frequency alteration mapping for extraoperative localization of speech cortex. Neurosurgery. 2010; 66:E407–E409. [PubMed: 20087111]

60. Yetkin FZ, Mueller WM, Morris GL, McAuliffe TL, Ulmer JL, Cox RW, et al. Functional MR activation correlated with intraoperative cortical mapping. AJNR Am J Neuroradiol. 1997; 18:1311–1315. [PubMed: 9282861]

61. Zanos S, Miller KJ, Ojemann JG. Electrocorticographic spectral changes associated with ipsilateral individual finger and whole hand movement. Conf Proc IEEE Eng Med Biol Soc. 2008:5939–5942. [PubMed: 19164072]

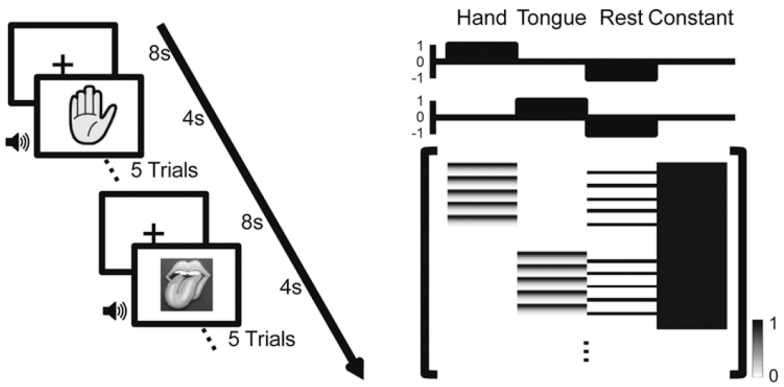

Fig. 1.

Left: Schematic diagram of the experimental setup. Surgical patients with implanted subdural electrodes performed hand or tongue movement tasks in 20-second blocks interleaved with 8-second rest blocks. The type of movement (hand or tongue) was indicated by a visual cue displayed on the screen throughout the block. In each task block, the patient grasped the hand contralateral to the side of electrode implantation, or stuck out his tongue immediately following an auditory cue (duration 0.2 seconds, average interstimulus interval 4 seconds). Each block involved only one type of movement. **Right:** The GLM design matrix. The *upper 2 plots* show the contrast vectors of the hand and tongue movement tasks. The *lower graph* depicts the design matrix, with each row corresponding to one sample point of the ECoG. The full design matrix contains 4 columns. The first 2 columns represent the hand and tongue movement; the third column represents the rest condition, and the fourth is the constant. The 2 task columns were obtained by replacing the first 3 seconds of each trial with a high gamma response template. s = seconds.

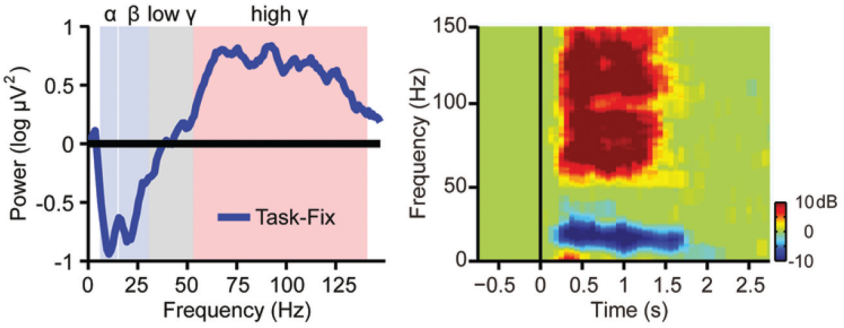

Fig. 2.

Left: The relative power (task/rest) of the ECoG signal recorded from the representative electrode during movement (from 0.3 to 1.3 seconds after the auditory cue onset). The representative electrode was chosen if the patient showed or reported symptoms related to the sensory motor cortex when stimulated with the minimum current intensity during the ECS test. The *blue curve* represents the relative power spectra averaged across all 17 patients. The movement task induced a significant power increase in the high gamma band but a decrease in the alpha (8–13 Hz) and beta (15–30 Hz) bands. The power in the low gamma band did not show any significant change. **Right:** The time-frequency plane was divided into small time-frequency bins (each bin is 15 msec ×1 Hz). The power spectra in the time-frequency bins showing significant task versus rest difference were averaged across all subjects. The modulation effect of the movement tasks was clearly demonstrated in the high gamma band and some of the low-frequency bands.

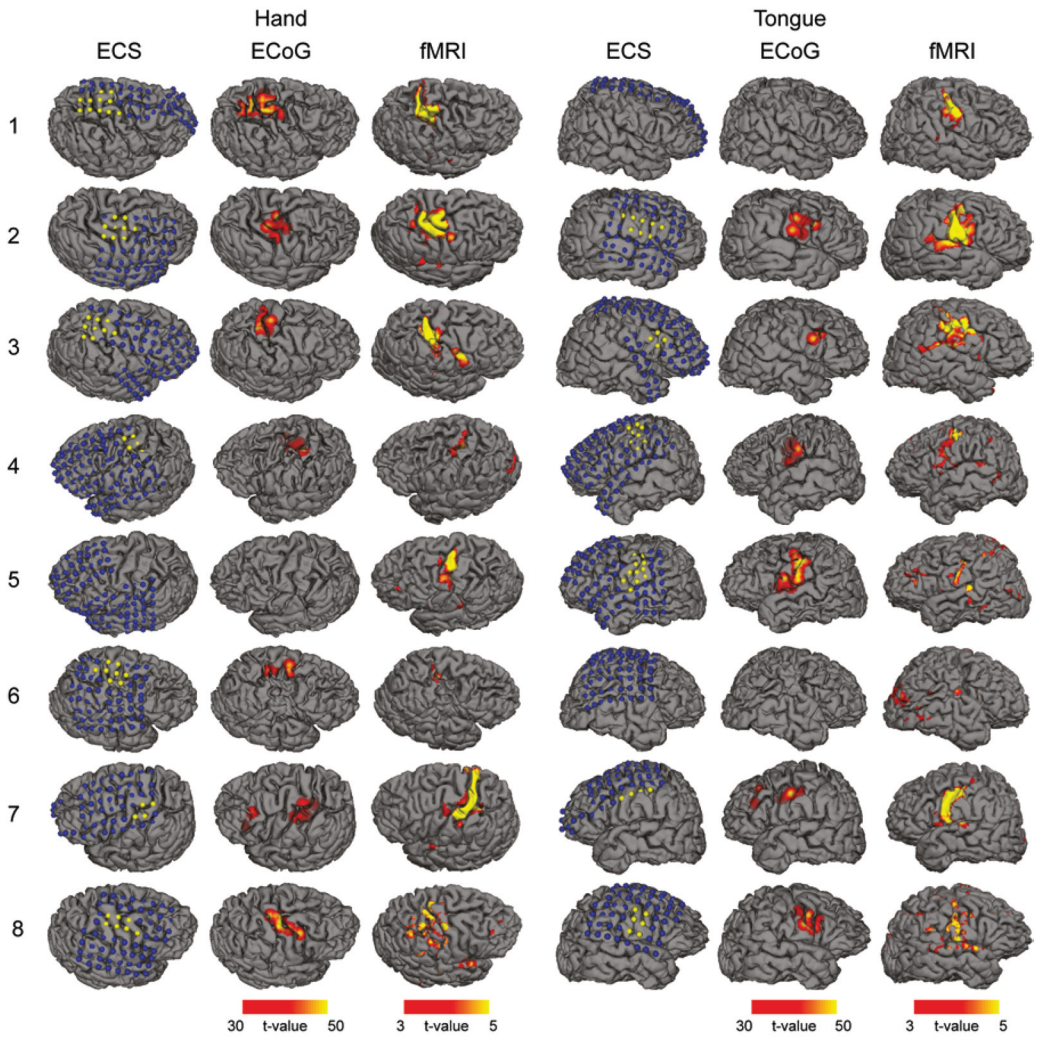

Fig. 3.

Hand and tongue motor areas localized by ECS, ECoG, and fMRI. The mapping results were projected to each individual's brain surface reconstructed from the T1-weighted MR images. Each row represents the results obtained in 1 patient. The number on the left is the case number as shown in Table 1. The left 3 columns illustrate the hand motor regions mapped by ECS, ECoG, and fMRI, respectively. The right 3 columns are the maps of the tongue motor regions. The *blue dots* in the ECS maps indicate negative electrodes (no symptoms related to sensory motor cortex reported when stimulated) and the *yellow dots* indicate positive electrodes. The ECoG results were the t-values of all electrodes determined by the GLM rendered on the cortical surface. The fMRI activation maps were also the t-values determined by the GLM. The ECoG maps were highly consistent with the ECS findings and were more localized than fMRI results.

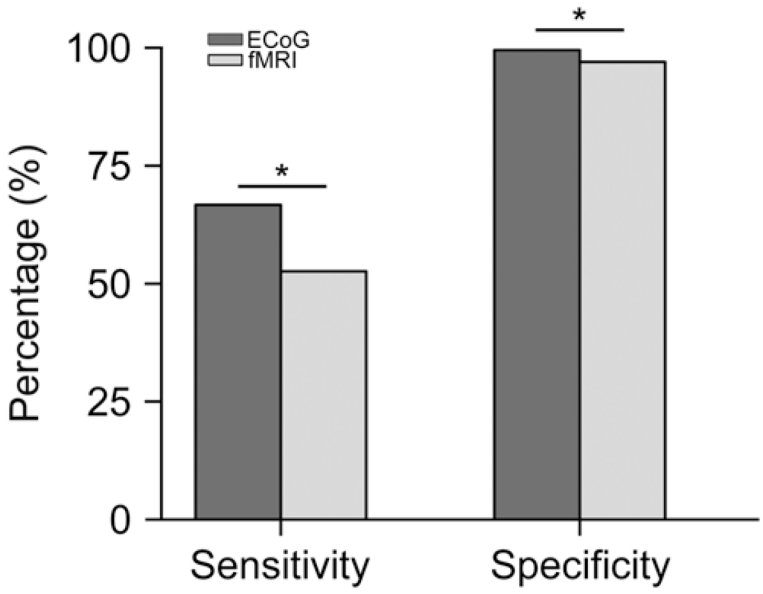

Fig. 4.

Overall sensitivity and specificity of ECoG and fMRI mapping. To determine the sensitivity and specificity, ECS results were used as the reference. The sensitivity and specificity in each patient are listed in Table 2. The overall percentage is computed as the total number of electrodes belonging to A, B, C, or D conditions (defined in Table 2) over all tasks and patients (17 patients for ECoG, 8 patients for fMRI). Compared with fMRI, ECoG mapping results are significantly more consistent with the ECS findings. *$p < 0.05$, paired t-test.

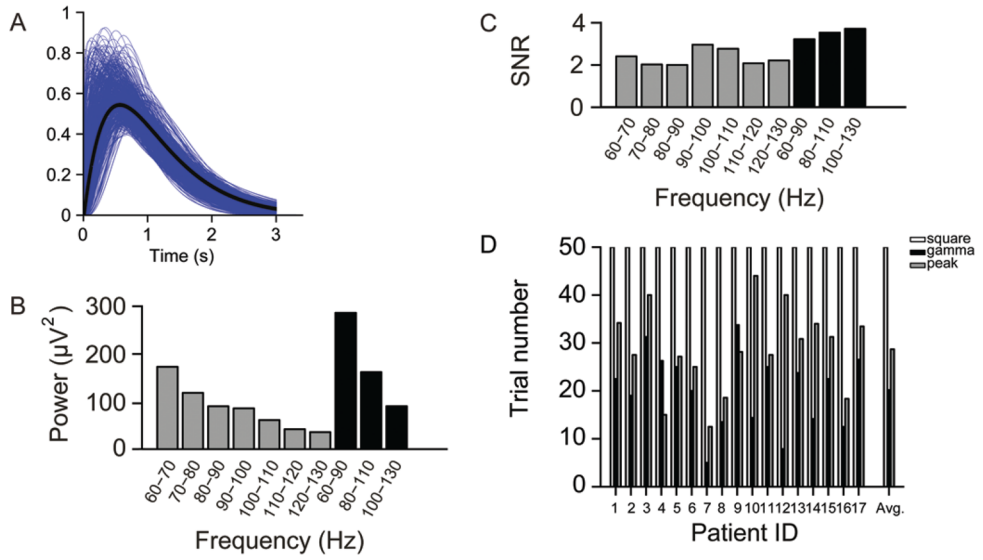

Fig. 5.

A: A high gamma response template was obtained by averaging the single-trial gamma-band activity. The *blue curves* are the fitted gamma functions of single trials recorded from the representative electrodes. The *black curve* is the high gamma response template derived from averaging the blue curves. **B:** The gamma band was separated into multiple subbands, and the mean power in these subbands was averaged across all trials/tasks/subjects. For each trial, the mean power during the time window of 0–2 seconds was calculated. Compared with other subbands, the 60-to 90-Hz band has the highest power during movement tasks. **C:** The broadband (30-Hz bin) high gamma envelope has a greater signal-to-noise ratio than the narrow band (10-Hz bin). The broadband high gamma activity, especially between 60 and 90 Hz, has a greater t-statistic value than the other subbands within the same ECoG data set. **D:** Using the gamma template, fewer trials are needed to achieve the same performance than when the square template or the peak template are used. On average, the gamma template needs 20 trials, the square template needs 50 trials, and the peak template needs 29 trials for the same performance. SNR = signal-to-noise ratio. Patient ID = case number (Table 1).

TABLE 1

Summary of patient demographic and clinical characteristics*

Case No.	Age (yrs), Sex	Age (yrs) at Sz Onset	Sz Frequency	Sz Type	Dx	Hand	Grid	No. of Electrodes
1	14, M	3	4/day	CP w/ G	rt fr	rt	rt fr, rt par	76
2	24, F	14	8/mo	CP	rt fr	rt	rt fr, rt par	68
3	17, F	8	3/day	CP w/ G	rt fr	rt	rt fr, rt par, rt temp	96
4	12, M	10	2/day	CP	lt fr	rt	lt fr, lt par, lt temp	116
5	20, M	12	1/mo	CP	lt fr	rt	lt fr, lt par, lt temp	96
6	20, F	10	2/mo	CP	rt par	rt	rt par	64
7	27, F	18	2/mo	CP	lt par	lt	lt par	64
8	22, F	16	5/day	CP	rt fr	rt	rt fr, rt par	64
9	21, M	8	2/mo	CP	lt fr	rt	lt fr, lt par	64
10	15, F	4	3/mo	CP	lt temp	rt	lt fr, lt temp	64
11	18, M	9	1/mo	CP	lt fr	rt	lt fr, lt par	58
12	29, M	5	4/mo	CP	rt fr	rt	rt fr, rt par	76
13	16, M	9	1/day	CP	lt fr	rt	lt fr, lt par, lt temp	96
14	20, F	15	1/day	CP	rt fr	rt	rt fr, rt par	32
15	15, M	1	1/mo	CP w/ G	rt temp	rt	rt fr, rt par, rt temp	96
16	9, M	8	3/mo	CP w/ G	lt fr, lt temp	rt	lt fr, lt par, lt temp	96
17	15, M	8	8/day	CP	lt fr	rt	lt fr, lt par	46

*CP = complex partial; Dx = diagnostics; fr = frontal; G = generalization; par = parietal; Sz = seizure; temp = temporal.

TABLE 2

Sensitivity and specificity of ECoG and fMRI*

	Sensitivity (%)		Specificity (%)	
Case No.	**ECoG**	**fMRI**	**ECoG**	**fMRI**
1	90.9	36.4	100	98.6
2	59	70.8	100	95
3	52.8	22.2	100	97.2
4	71.3	38.8	100	98.6
5	66.7	50	100	98.4
6	62.5	37.5	100	98.4
7	87.5	87.5	96.7	97.5
8	77.4	70.2	100	89.5
9	69.4		100	
10	75		96.8	
11	62.5		100	
12	75		100	
13	58.3		98.9	
14	37.5		100	
15	25		100	
16	75		99.5	
17	62.5		100	

*The percentage value given for each patient is the average of the hand and tongue movement tasks.

TABLE 3

The pros and cons of ECS, ECoG, and fMRI

Criterion	ECS	ECoG	fMRI
sensitivity	gold-standard	66.70%	52.50%
specificity	gold-standard	99.60%	97.00%
time cost	1–2 hrs	5–10 mins	10–15 mins
invasiveness	yes	yes	no
risk	after-discharge Sz	minimal	minimal
additional equipment	stimulator	none	MRI scanner